# Adaptation of the machine to the new geological conditions – excavation unit redesign and optimization

Jakub ANDRUSZKO, Przemyslaw MOCZKO, and Damian PIETRUSIAK*

Department of Machine Design and Research, Wroclaw University of Science and Technology,
ul. Ignacego Lukasiewicza 7/9, 50-371 Wroclaw, Poland

**Abstract.** The paper presents and sums up the research and technical aspects of the modernization of the cutting tool of the dredger. Improper adjustment of the cutting elements not adjusted to the characteristics of excavated material is not an uncommon situation, causing versatile geological conditions. Relocation of the machines from one pit to another may result in the significant influence on the excavation process (wear, output, etc.). Common practice is the field try and error approach to obtain desired machine performance. In the paper authors present the approach with aid of cutting-edge technologies. Coupled DEM and kinematic simulations supported by the reverse engineering technologies of laser scanning were the fundamental drivers for final adjustments of the cutting tool at its present operational conditions.

**Key words:** dredger; rigid-body dynamic; 3D scanning; discrete element method; finite element method.

## 1. Introduction

Adjustment of the cutting tool on the excavating head/wheel plays a significant role for the machine output and the wear process of the cutting tools. Industrial practice as well as literature study indicates bucket/cutting wheels as one of the most exposed to the damage, other than for example structural and undercarriage components of the machinery [1, 2]. Papers [3, 4] present design, technological and fatigue cause of excavating unit damage. Literature review of [5, 6] gives an example of shaping cutting tools with the use of numerical simulations.

Relocation of the machine leads to its operation in not preferable geological conditions. As a result, predefined geometry of cutting elements dedicated to specific geological conditions is not the optimal one. From the technical point of view the increase of excavation resistance and wear acceleration is observed. As a consequence, maintenance actions must be taken more often increasing the total cost of operation. Also, the rise of the excavation resistance causes a drop in the output rate. Total down time (due to the additional maintenance), output drop, increased maintenance costs lead to the significant total cost increase. It rises doubts about the economic justification of the operation.

The solution of this situation is an adaptation of the excavation tools and excavation parameters to the actual operational conditions. In many cases, this is realized by the try and error method which can, as a consequence, lead to the positive or negative change. Depending on the characteristics of the excavated/moved material, small workshop adjustments may not give the desired result. More detailed analysis of trajectories may be necessary [7].

Authors of this paper present research based, step by step process of identification and modification of the excavation unit in purpose of its adaptation to actual working conditions. The object of investigation was a cutter head of the sand dredger [8] presented in Fig. 1. The analyses were supported by the reverse engineering as well as computed aided design and numerical simulation tools [9].



Fig. 1. Suction dredge barge

## 2. Problem identification

For the purpose of defining the root cause of the excavation problem the identification of real operational conditions, parameters and resistance is crucial. At first, the positioning system of the bagger must be properly defined. In the presented case the position of the bagger is controlled with steel ropes. Three of these ropes keep the global position which remains stable during excavation. Two side ropes control the slewing of the bagger with respect to the fixed point (defined by the global positioning ropes). In Fig. 2 the positioning rope system is presented.

*e-mail: damian.pietrusiak@pwr.edu.pl

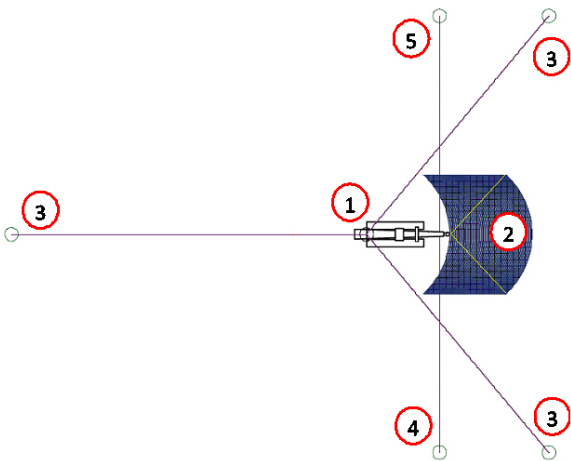J. Andruszko, P. Moczko, and D. Pietrusiak

Fig. 2. Scheme of the dredger positioning: 1 – dredger, 2 – operation field, 3 – global positioning ropes, 4 – operation (slewing) positioning ropes

Analysis of the winch operation pressure and the machine operation gives direct indication of the overload of the winches. The interrupted machine operation results with the output significantly below the expected level. The trace of the pressure on the left and right slewing winch as well as the cutterhead pressure, measured experimentally, are presented in Fig. 3. The detailed description of the overloading problem is presented in the paper [10]. In general, one can observe that the operation process is very unstable with big alternations on the wheel load and loads on the slewing.
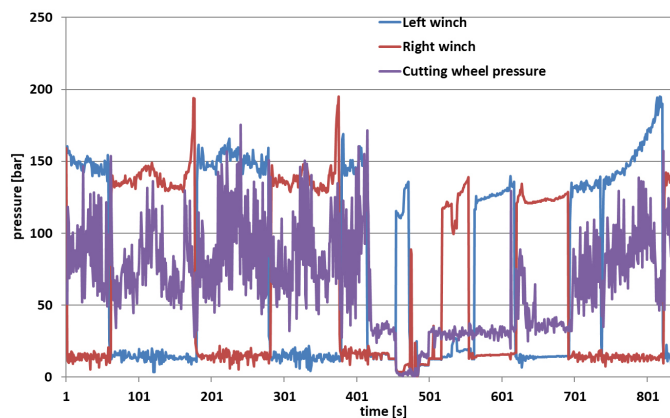


Fig. 3. Cutterhead winch pressure and cutting wheel pressure trace

## 3. Author's method of problem solving

The methodical approach, in purpose to solve the presented problem, is defined by the following steps:

- Definition of the actual geometry of the wheel and teeth
- Identification of the trajectories of the cutting teeth
- Identification of the load distribution on the cutting elements
- Optimization

- Assessment
- Final adjustments

The listed steps are described in the following subchapters.

**3.1. Definition of the actual geometry of the wheel and teeth.** Due to the many workshop try and error adjustments, which were not fully documented and coordinated, the actual position and shape of the cutting elements were identified with use of reverse engineering 3D laser scanning technology (Fig. 4).



Fig. 4. Geometry scanning

In the methodology of this process, a terrestrial laser 3D scanner was used, which identifies the position of points in any spatial coordinate system X, Y, Z. During this process, the scanning density of the object is defined. and the corresponding incremental interval of the horizontal and vertical angles, which, together with the measured distance, are then used to calculate the X, Y, Z rectangular coordinates of each point in the point cloud. As a result, rectangular coordinates are obtained from the polar coordinates. The coordinates of the points can be determined in the local scanner coordinate system and also in the coordinate system defined by the user.

The full "field of view" of the scanner head covers 360°in horizontal and 270°in vertical direction. The accuracy of the measurement depends on the distance and type of the scanned object, i.e., its color, surface roughness, reflectivity (albedo coefficient) and the number of scans performed (overlapping point clouds of the same detail). Measurement accuracy in the field may be affected by wind as well.

The result of a single scan is a cloud of points scattered in space in relation to the current position of the scanner. The position of each point is exactly positioned relative to the vertical direction, with the accuracy of one arc second, thanks to dynamic measurement of the deviation from the vertical axis of the scanner. The final result of the measurements is the combined point cloud from all scans with the use of permanent markers visible during each scan. Such point cloud is the basis for the assessment of the geometry of the examined structure. Depending on the need, the 3D geometry can be built on the point cloud, that enables detailed geometry or FEM analyses (Fig. 5).

It is worth noting, that in case of the modernization of existing objects, it is a common situation that technical documentation and actual geometry discrepancy are present. Skipping

2

Bull. Pol. Acad. Sci. Tech. Sci. 69(3) 2021, e137122
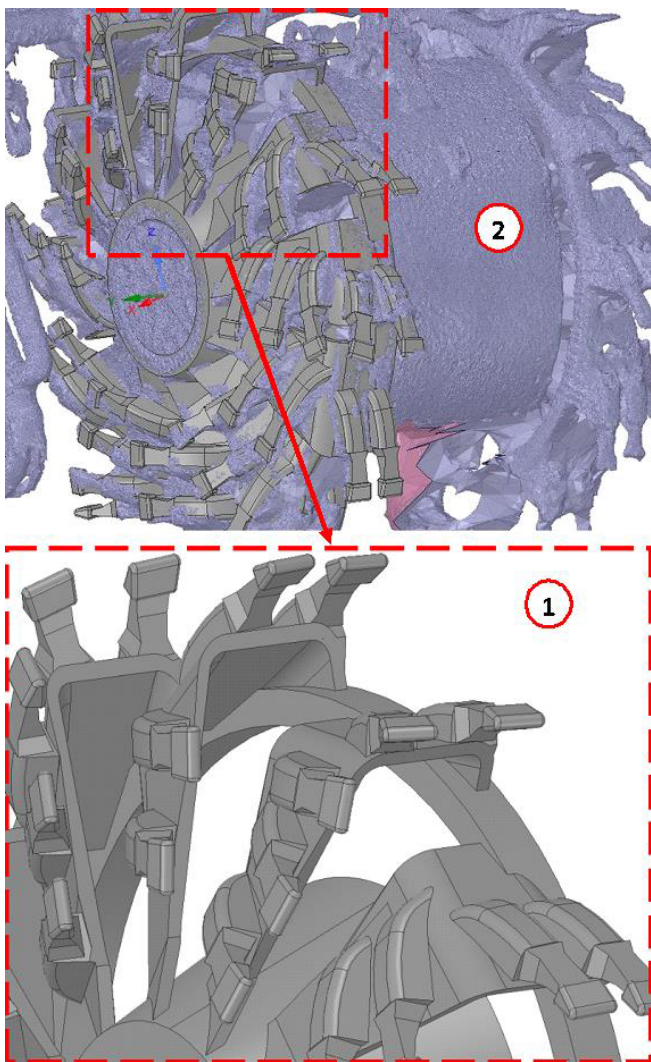
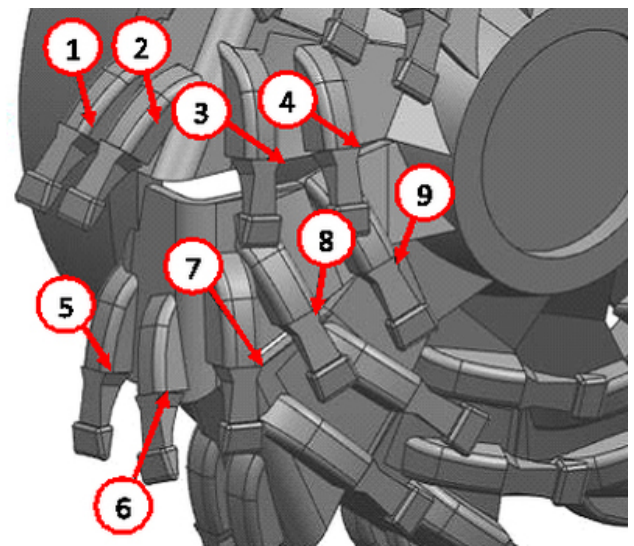Fig. 5. 3D virtual model (1) based on 3D scan model (2)



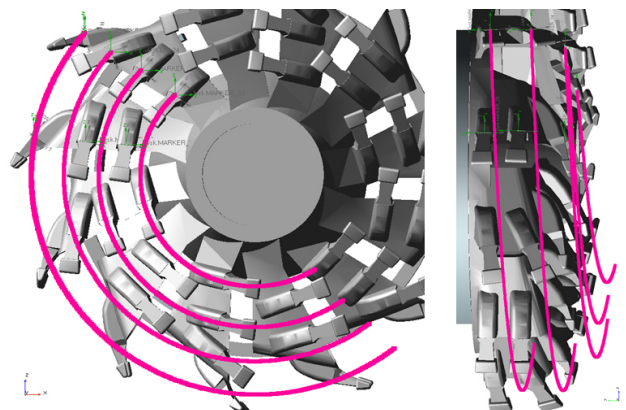Fig. 6. Selected teeth for the trajectory analysis



Fig. 7. Teeth trajectories of current model

the stage of actualization may have big influence on the final results of the optimization. Moreover, it reveals if the preliminary assumptions and design are correct. More details about the geometry recovery are presented in the paper [10].

**3.2. Identification of the trajectories of the cutting teeth.**
Having the actual geometry, the trajectory analysis of cutting element can be done. Due to the fact that cutting teeth are placed uneven on the buckets/wheel, the analysis was performed with two buckets simultaneously. This approach gives the possibility to assess the position of each tooth separately as well as the possible mutual influence of the trajectories of teeth. The parameters for presented analysis were as follows: slewing – 5 m/min, wheel speed – 28 rpm. In Fig. 6 direct indication of teeth taking part in the simulation is presented.

Figure 7 presents the trajectory of selected teeth. Comprehensive discussion about trajectory analysis can be found in the paper [10].

Each tooth was analyzed under the inclination angle with respect to the surface tangent to the trajectory trace [10]. The

analysis was done separately in radial and axial direction. Superposition of those two analyses gives the resultant trajectory of the cutting tool. Graphical example of the inclination angle definition is presented in Fig. 8.
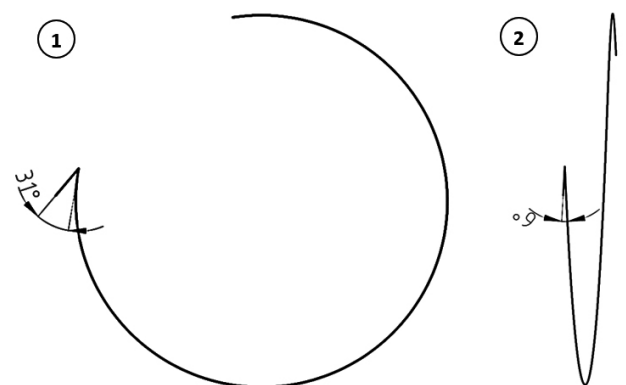


Fig. 8. Teeth trajectories – tooth deviation angles – teeth nr 1: 1 – radial direction angle, 2 – axial direction angle

Bull. Pol. Acad. Sci. Tech. Sci. 69(3) 2021, e137122

3

J. Andruszko, P. Moczko, and D. Pietrusiak

### 3.3. Identification of the load distribution on the cutting elements.

The third step of the presented approach is the numerical simulation to identify the load distribution, material fragmentation and total resistance check. The simulation was based on Discrete Element Method. The developed model was validated on the basis of the measured values of the excavation resistance [11].

In the discrete approach, each particle of material is modeled separately, and the whole material is represented as an idealized set of particles. The general behavior of the set of particles is, due to interactions, between the molecules. In DEM, by the use of contact detection algorithms and the use of appropriate contact models, the forces acting on the particles are calculated (Fig. 9). Accelerations, velocities, and positions are then computed using Newton's laws of motion and numerical integration. Each particle has 6 degrees of freedom, and as a result can have two kinds of motion: translational and rotational. In DEM simulations, Newton's second law is used to calculate the translational and rotational acceleration, which are then numerically integrated over a time interval to update the velocities and positions of the particles [12].
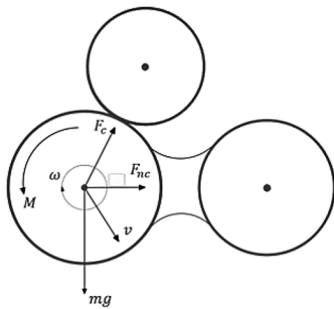


Fig. 9. Example of forces acting on a 2D discrete particle. Same principles govern 3D DEM simulations with 6 d.o.f. [12]

The rotational motion is calculated based on the following equation [14]:

$$I\frac{\mathrm{d}\omega}{\mathrm{d}t} = M,\qquad(1)$$

where $I$ is the moment of inertia, $\omega$ is the angular velocity, $M$ is the resultant contact torque acting on the particle, $t$ is time. The translational motion is calculated based on the following equation [12]:

$$m\frac{\mathrm{d}v}{\mathrm{d}t} = F_g + F_c + F_{nc},\qquad(2)$$

where $v$ is the translational velocity of the particle, $m$ is the mass of the particle, $F_g$ is the resultant gravitational force acting on the particle, $F_c$ and $F_{nc}$ are the resultant contact and noncontact forces between the particle and surrounding particles or walls. The accelerations are numerically integrated over a time step to update particle velocities and positions [12]:

$$x(t+\Delta t) = x(t) + v(t)\Delta t,\qquad(3)$$
$$v(t+\Delta t) = v(t) + a(t)\Delta t,\qquad(4)$$

where $v(t)$ is velocity, $x(t)$ is the position, $a(t)$ is the accelerate of a particle at a given time $t$, $\Delta t$ is the time step (Fig. 10). Rotational velocity and particle orientations are updated in a similar manner [12].
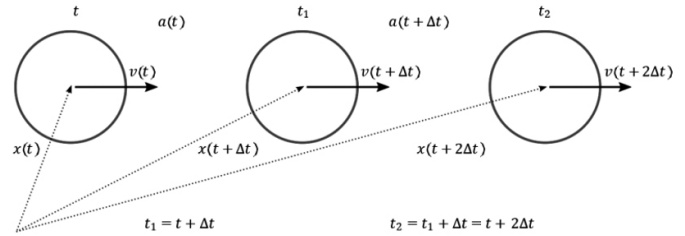


Fig. 10. Single element motion calculation in terms of acceleration, velocity and position in DEM [12]

Based on the literature data [7, 13–16], the basic properties of the excavated material – quartz – and the size of the discrete element were determined. Material properties and parameters of the discrete elements are presented in the Table 1 below.

Table 1
Material properties and parameters of discrete elements, where: $R_p$ – physical radius, $R_c$ – contact radius, $\rho$ – density, $v$ – Poisson's ratio, $E$ – Young modulus

| Material properties and parameters of discrete elements | | | | |
|---|---|---|---|---|
| $R_p$ [mm] | $R_c$ [mm] | $\rho$ [kg/m$^3$] | $v$ [−] | $E$ [Pa] |
| 5 | 6 | 2700 | 0.25 | 2.5E9 |

The Hertz–Mindlin with bonding contact model was used. In this model the normal force component is based on Hertzian contact theory [16]. The tangential force model is based on Mindlin-Deresiewicz work [17]. Both normal and tangential forces have damping components where the damping coefficient is related to the coefficient of restitution as described in [18]. The tangential friction force follows the Coulomb law of friction model as in, for example in [19]. The rolling friction is implemented as the contact independent directional constant torque model [18]. Additionally, when using bonding, contact model bonds spheres together. The bond is broken when the normal and tangential shear stresses exceed some predefined value [15]:

$$\sigma_{\max} < \frac{-F_n}{A} + \frac{2M_t}{J}R_B,\qquad(5)$$

$$\tau_{\max} < \frac{-F_t}{A} + \frac{2M_n}{J}R_B.\qquad(6)$$

These bond forces/torques are in addition to the standard Hertz–Mindlin forces [15].

To obtain bonding contact parameters, a series of numerical simulations was performed. To represent the mining process, a soil block consisting of 451 997 particles was created.

4

Fig. 11. DEM simulation model

As mentioned, model validation was based on the excavation resistance measured data. Due to the alternating character of the cutting forces, the validating parameter was the Root Mean Square value of the excavation force trace [10]. Value (7) is the obtained on the measured experimental data. Value (8) gives the resistance level derived on the basis of tuned model:

$$RMS_{S0cutterhead} \cong 11\,623\,\text{Nm}, \tag{7}$$

$$RMS_{S0cutterhead} \cong 12\,102\,\text{Nm}. \tag{8}$$

S0 is current solution of cutterhead. The difference between (7) and (8) is roughly only about 4%. The trace of the torque in the numerical simulation is presented in Fig. 12. The indicated time intervals present wheel run up, stabilization of the excavation and interval of stable operation selected for validation, respectively.
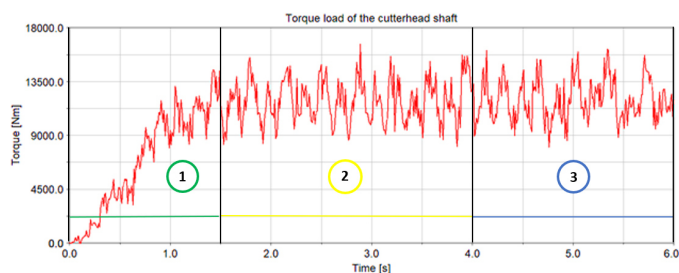


Fig. 12. Torque load of the cutterhead drive shaft – current solution of the cutterhead: 1 – start of the wheel, 2 – stabilization of the cutting process, 3 – determining the RMS value

The root mean square value of the torque of slewing motion obtained in numerical analysis is:

$$RMS_{S0ladder} \cong 818\,890\,\text{Nm}. \tag{9}$$

As a result, the following parameters were obtained for bonded-type contact.

Using obtained parameters, 2 091 528 contact connections between the molecules were obtained.

Table 2
The Hertz–Mindlin with bonding contact parameters, where: $C_n$ – normal stiffness, $C_s$ – shear stiffness, $\sigma_{crit}$ – critical normal stress, $\tau_{crit}$ – critical shear stress, $R_{nond}$ – bonded disc radius

| The Hertz–Mindlin with bonding contact parameters | | | | |
|---|---|---|---|---|
| $C_n$ [N/m³] | $C_s$ [N/m³] | $\sigma_{crit}$ [Pa] | $\tau_{crit}$ [Pa] | $R_{nond}$ [mm] |
| 1E9 | 5E8 | 6.5E5 | 6.25E5 | 6 |

**3.4. Optimization.** The recovered 3D geometrical model identified trajectories and the discrete numerical model for bulk material simulation is a proper basis for optimization process. The first introduced change was the new adjustments of the cutting teeth with respect to the angels and trajectories. The general information about the cutting elements and earth moving machinery design is presented in the positions [7, 14, 20–22]. More detailed investigation of the excavation resistance with respect to the teeth angel is presented in position [10]. The field based experience is presented in positions [23–25]. With the combination of both theoretical and experimental knowledge the solution (Fig. 13) of the new placement of the cutting teeth on the buckets was proposed.
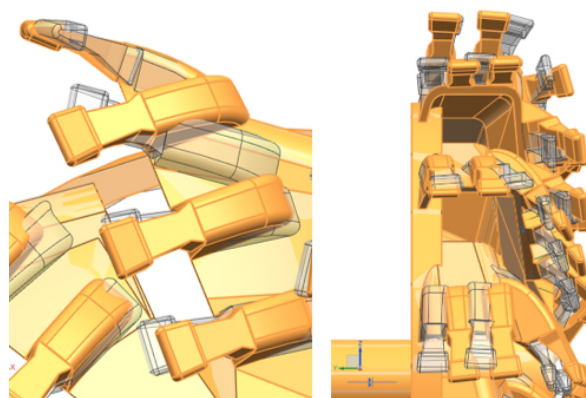


Fig. 13. The new arrangement of the teeth

In Fig. 14 the numerical discrete element simulation, with new position of the cutting tools is presented.
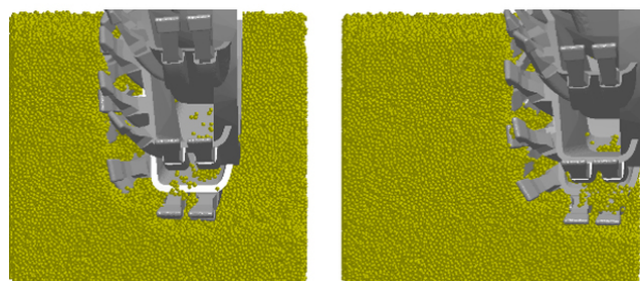


Fig. 14. Example of the mining process simulation – optimized solution

For the purpose of evaluating the influence of the change in the cutting elements setup, new values of the resistance

Bull. Pol. Acad. Sci. Tech. Sci. 69(3) 2021, e137122

5

force were determined with use of the DEM model. Figure 15 presents the trace of the torque on the cutting wheel and Fig. 16 presents the torque required for slewing.
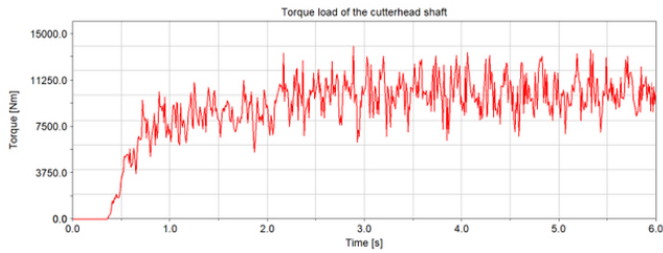


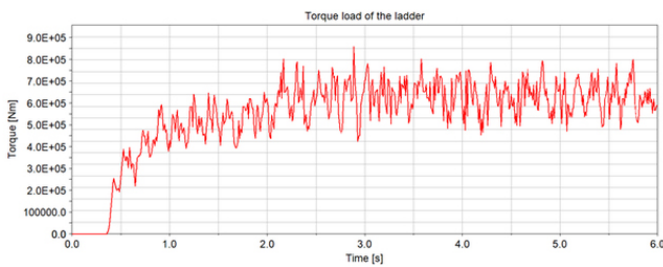Fig. 15. Torque load of the cutterhead drive shaft – optimized solution



Fig. 16. Torque load of the slewing motion – optimized solution

The effective reference values of the obtained characteristics were determined. Torque on the cutterhead drive shaft equals:

$$\text{RMS}_{\text{S1cutterhead}} \cong 10\,316\,\text{Nm}, \tag{10}$$

Torque on the ladder (slewing motion) equals:

$$\text{RMS}_{\text{S1ladder}} \cong 631\,560\,\text{Nm}. \tag{11}$$

Due to the fact that optimized position of the cutting teeth was significantly different from the original one, the new shape of cutting wheel with buckets must have been developed. As previously, simulations with new geometry of the wheel and cutting tools setup, were run to assess the influence on the resistance forces of excavation. Figure 17 presents the simulation with new geometry of the wheel and new shape of the teeth which was optimized to the new position on the wheel.
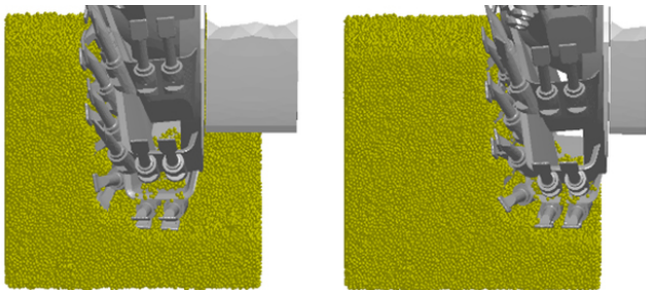


Fig. 17. Example of the mining process simulation – the new solution of bucket wheel

Traces of the obtained torque values of the optimized solution are presented in Figs. 18 and 19.
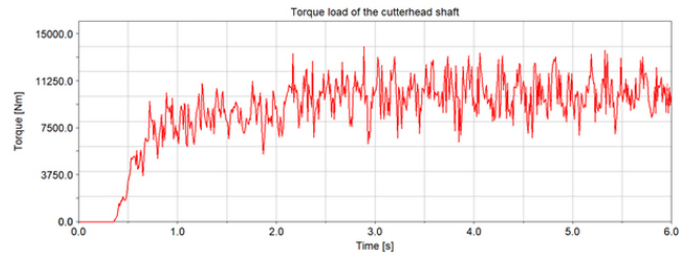


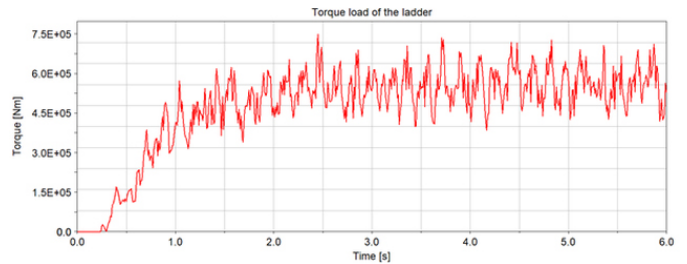Fig. 18. Torque load of the cutterhead drive shaft – new solution



Fig. 19. Torque load of the cutterhead drive shaft – new solution

As previously, the effective reference values of the obtained characteristics were determined in stable interval of the trace. Torque of the cutterhead drive shaft equals:

$$\text{RMS}_{\text{S2cutterhead}} \cong 10\,394\,\text{Nm}, \tag{12}$$

Slewing torque equals:

$$\text{RMS}_{\text{S2ladder}} \cong 565\,440\,\text{Nm}. \tag{13}$$

**3.5. Assessment of the solutions.** After the numerical simulations, it was possible to evaluate all solutions. All loads for the bucket wheel are shown in Figs. 20 and 21, and for the slewing torque in Figs. 22 and 23. Figures 21 and 23 show fragments of graphs for which RMS values were determined.
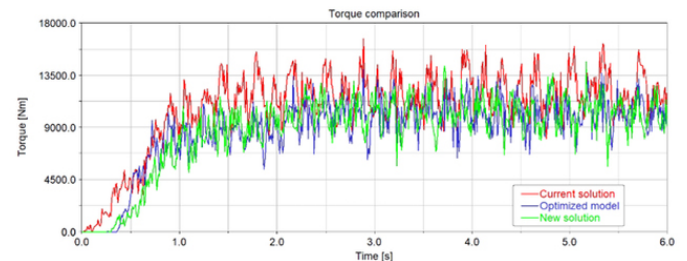


Fig. 20. Torque load of the cutterhead drive shaft – comparison

The determined RMS values of the loads are listed in Table 3.

Comparing the determined RMS values of loads, the reference is the value for the simulation with the solution of teeth and bucket wheel currently used on the dredger. The differences in percentages, between the solutions, are shown in Table 4.

6

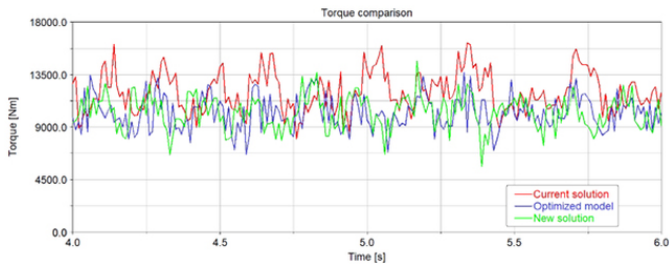Bull. Pol. Acad. Sci. Tech. Sci. 69(3) 2021, e137122

Fig. 21. Torque load of the cutterhead drive shaft – comparison – RMS values



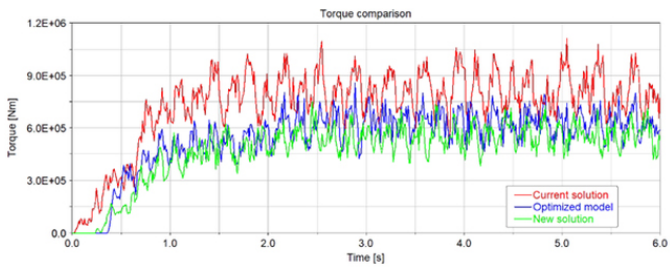Fig. 22. Torque load of the ladder – comparison



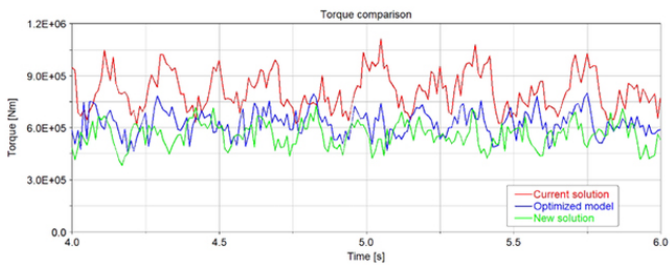Fig. 23. Torque load of the ladder – comparison – RMS values

tation, after the cutting tool pass for current solution and new solution, were compared and are shown in Figs. 24 and 25.
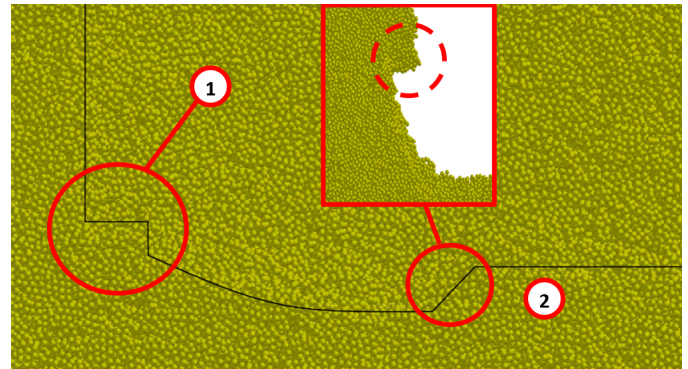


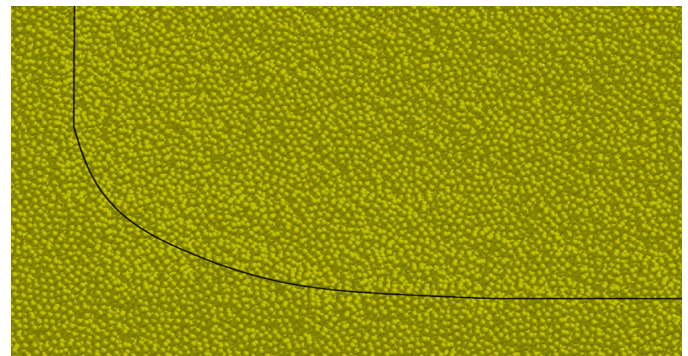Fig. 24. Soil block after the cutting process – current solution of cutterhead



Fig. 25. Soil block after the cutting process – new solution of cutterhead

Table 3
Torque comparison

| Move | Torque RMS [Nm] | | |
|---|---|---|---|
| | Current solution | Optimized model | New solution |
| Cutterhead rotation | 12 102 | 10 316 | 10 394 |
| Dredger slew | 818 890 | 631 560 | 565 440 |

Table 4
Differences, in percent, between the solutions

| Move | Relative torque change [%] | | |
|---|---|---|---|
| | Current solution | Optimized mode | New solution |
| Cutterhead rotation | 100 | 85 | 86 |
| Dredger slew | 100 | 77 | 69 |

The additional parameter of the solution assessment is the cutting process itself. The obtained results of the soil fragmen-

In the case of the current solution of the cutterhead, the soil block after the tool pass is unfavorable. Point 1 in Fig. 24 indicates that the teeth on the wheel are misplaced. In this point, the material has not been detached along its entire length. The efficiency of the cutting process is unsatisfactory. Point 2 represents the unbonded material and this is because there is no tooth on the bucket wheel at this point. In the soil block presented in Fig. 25, it can be noticed that the appropriate spacing of the teeth and the change in their number resulted in not only reducing the loads, but also increasing the efficiency of the process by collecting all the material.

**3.6. Final adjustments and shaping.** Once the geometrical and operational parameters were determined, the strength checkout is required to assure safe and reliable operation. A discrete model based on 820206 finite elements spanned on 1265092 nodes was built. Linear structural analyzes were performed. In the analyzed case, the influence of the position of the teeth on the buckets on the wheel effort was checked. Figure 26 presents the simulations performed simultaneously with the development of the new shape and position of cutting tools. Simulations at that state may give additional crucial information about scale of the required changes. In the presented case,

Bull. Pol. Acad. Sci. Tech. Sci. 69(3) 2021, e137122

7

the new support for teeth was required both due to the positioning and strength requirements.
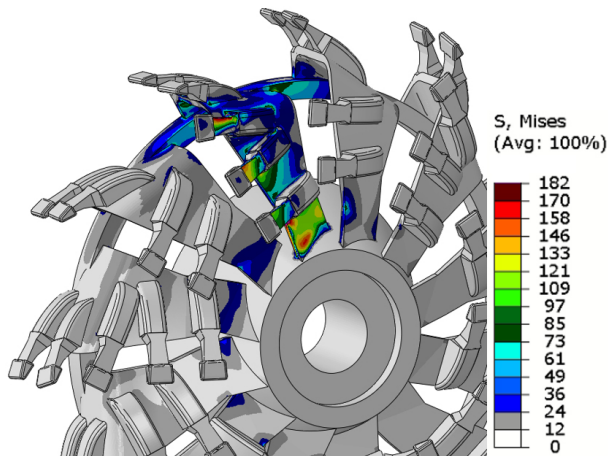


Fig. 26. Additional possibilities of the presented method – numerical simulations using FEM

In the end when final solution is defined, detailed simulations, including fatigue resistance, should be performed. The final, optimized shape of the new wheel and cutting elements is presented in Fig. 27.
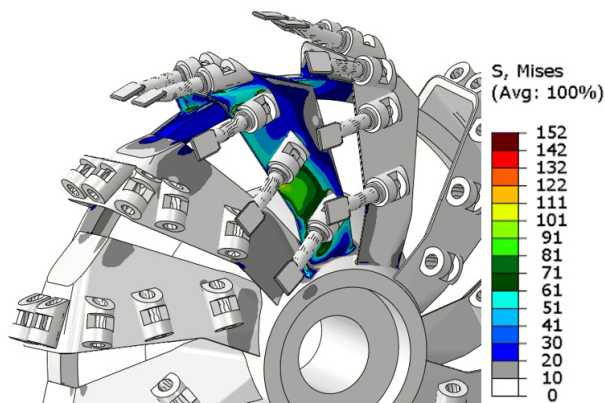


Fig. 27. Optimized shaped of the wheel and cutting tools

## 4. Conclusions

Operation in the geological conditions to which the machine was not designed, requires adaptation which may require detailed analysis. Profit from such work is the optimization of the technological process and ensuring its high efficiency, often higher than before the modernization. This is particularly important in highly energy-consuming processes, where the technological equipment used requires a large amount of energy. In such a case, even a few percent improvement in the efficiency gives significant financial savings, and also allows to reduce the negative impact on the environment, due to lower specific energy consumption (e.g., energy consumption per ton of excavated material or cubic meter of final product in the technological process). In order to be able to carry out such a process of adapting and modernizing the existing machine, it is necessary to conduct a series of simulation and experimental tests.

These activities define the method developed by the authors of this paper. The use of the method is presented on the example of the process of underwater mining of sand by the cutting head of the dredger. For this purpose, the following activities were conducted:

- 3D scanning of the existing design, which allows the assessment of the correctness of the construction in accordance with the design assumptions and creation of a virtual 3D model serving as an input for numerical analyzes.
- Identification or measurements of loads acting on the machine before modernization.
- Numerical simulations based on DEM, in the scope of:
  - validation of the numerical model with the use of the identified operational parameters of the existing design,
  - assessment of the correctness of the adopted type of tooth,
  - assessment of the correctness of the distribution of teeth on the bucket wheel in terms of the number of teeth and cutting angles,
  - development of a new solution or optimization of the existing one based on the adopted criteria and process optimization assumptions.
- Numerical simulations based on FEM, in the scope of:
  - Verification of the new solution in terms of ultimate and fatigue strength
  - Optimization of the above parameters.

The use of the developed method in the process of modernization of the cutting head of the dredger to the new operating conditions (increasing the cutting resistance), was carried out in two stages.

In the first stage, the existing cutting wheel design was optimized by changing the layout and correcting the cutting angles of the existing teeth. This resulted in an improvement in the efficiency of the cutting process by an average of 19%, which causes reduction of the cutting resistance while maintaining the output of the machine. Alternatively, it is possible to increase the output by using the obtained power reserve of the machine drives.

In the second stage, a new design for the cutting system of this machine was developed, dedicated to the current operating conditions. This allowed to improve the efficiency in relation to the initial variant of the mining process by an average of 22%.

The presented approach to the modernization process brings significant effects of improving the efficiency of the mining process, and thus it is fully justified from the economical and ecological point of view.

## References

[1] M. Saga *et al.*, "Experimental Determination of the Manson-Coffin Curves for an Original Unconventional Vehicle Frame", *Materials* 13, 4675 (2020), doi: 10.3390/ma13204675.

[2] J. Dizo *et al.*,"Development of a New System for Attaching the Wheels of the Front Axle in the Cross-Country Vehicle", *Symmetry-Basel* 12, 1156, (2020), doi: 10.3390/sym12071156.

[3] S. Bosnajk and N. Zrnic, "Dynamics, failures, redesigning and environmentally friendly technologies in surface mining systems", *Arch. Civ. Mech. Eng.* 12, 348–359 (2012).

[4] D. Danicic, S. Sedmak, D. Ignjatovic, and S. Mitrovic, "Bucket wheel excavator damage by fatigue fracture – case study", *Procedia Mater. Sci.* 3, 1723–1728, 2014.

[5] J. Peng, X. Liquan, L. Zheng, X. Liang, and Y Li, "Analysis On Layered Rock Cutting Process With Cutter Suction Dredger Based On Discrete Element Method", in *E-proceedings of the 38 th IAHR World Congress 09,* 2019, doi: 10.3850/38WC092019-0333.

[6] A. Amiadji, A. Baidowi, and R. Prayogo, "Development of Cutter Head Design in Cutter Suction Dredger with Thickness and Pitch Variation", *Int. J. Mar. Eng. Inn. Res.* 3(3), 93–108 (2019).

[7] K. Pieczonka, *Inżynieria maszyn roboczych. Cz. 1, Podstawy urabiania, jazdy, podnoszenia i obrotu*, Wroclaw University of Science and Technology Publishing House, 2009, [in Polish].

[8] R.N. Bray, A.D. Bates, and J.M. Land, *Dredging: A Handbook for Engineers*, Butterworth-Heinemann, 1996.

[9] M. Macko, Z. Szczepański, D. Mikołajewski, E. Mikołajewska, and S. Listopadzki, "The Method of Artificial Organs Fabrication Based on Reverse Engineering in Medicine", in *Proceedings of the 13th International Scientific Conference. RESRB 2016. Lecture Notes in Mechanical Engineering.* Springer, Cham, 2016, doi: 10.1007/978-3-319-50938-9_36.

[10] J. Andruszko, P. Moczko, and D. Pietrusiak, "The use of numerical methods in cutterhead dredger excavation unit optimization"*,* in *Proc. XXIII International Conference on Material Handling, Construction and Logistics, MHCL 2019*, 2019, pp. 141–146.

[11] I. Rojek, "Modelowanie i symulacja komputerowa złożonych zagadnień mechaniki nieliniowej metodami elementów skończonych i dyskretnych", *Prace Instytutu Podstawowych Problemów Techniki PAN*, pp. 119–146, 2007 [in Polish].

[12] A. Danesh, A.A. Mirghaseim, and M. Palassi, "Evaluation of particle shape on direct shear mechanical behavior of ballast assembly using discrete element method (DEM)", *Transport. Geotech.* 23, 100357 (2020).

[13] P. Siemaszko and Z. Meyer, "Static load test curve analysis based on soil field investigations", *Bull. Pol. Acad. Sci. Tech. Sci.*, 67(2), 329–337 2019 doi: 10.24425/bpas.2019.128607.

[14] K. Pieczonka, *Maszyny górnicze: Maszyny urabiające i ładujące do podziemnej eksploatacji złóż rud,* Wroclaw University of Technology Publishing House, 1981, [in Polish].

[15] H. Gilvari, W. de Jong, and D.L. Schott, "Breakage behavior of biomass pellets: an experimental and numerical study", *Comp. Part. Mech.* 2020, doi: 10.1007/s40571-020-00352-3.

[16] H. Hertz, "On the contact of rigid elastic solids and on hardness", *Ch 6: Assorted Papers*, 1882.

[17] R.D. Mindlin, "Compliance of Elastic Bodies in Contact", *J. Appl. Mech.* 16(3), 259–268 (1949).

[18] Y. Tsuji, T. Tanaka, and T. Ishida, "Lagrangian numerical simulation of plug flow of cohesionless particles in a horizontal pipe", *Powder Technol.* 71, 239–250 (1992).

[19] P.A. Cundall and O.D.L. Strack, "A discrete numerical model for granular assemblies", *Géotechnique* 29, 47–65 (1979).

[20] T. Rashi, K. Jeremy, and D. George, "Bucket trajectory classification of mining excavators", *Autom. Constr*, 31, 128–139 (2013).

[21] S. Blouin, A. Hemami, and M. Lipsett, "Review of resistive force models for earthmoving processes", *J. Aerosp. Eng.* 14(3), 102–111 (2001).

[22] S.M. Bosnjak, D.C.D. Oguamanam, and N.D. Zrnic, "The influence of constructive parameters on response of bucket wheel excavator superstructure", *Arch. Civ. Mech. Eng.* 15(4), 977–985, 2015.

[23] E. Rusiński *et. al.*, "Investigations And Modernizations Of Buckets Of Surface Mining Machines", *Eng. Struct.* 90, 29–37 (2015).

[24] D. Pietrusiak, P. Moczko, and E. Rusiński, "Recent achievements in investigations of dynamics of surface mining heavy machines", in *Proc. 24th World Mining Congress: mining in a world of innovation – proceedings*, 2016, pp. 295–308.

[25] J. Czmochowski, P. Moczko, D. Pietrusiak, G. Przybyłek, and E. Rusiński, "Selected Aspects of Technical Condition State Assessment of Spreaders Operating in Lignite Mines", in *Proc. Proceedings of the 13th International Scientific Conference Computer Aided Engineering*, 2016, pp. 89–98.

[26] E. Rusiński and J. Czmochowski, T. Smolnicki, *Zaawansowana metoda elementów skończonych w konstrukcjach nośnych,* Wroclaw University of Science and Technology Publishing House, 2000, [in Polish].

Bull. Pol. Acad. Sci. Tech. Sci. 69(3) 2021, e137122

9